

c+ production in Pb–Pb collisions at $\sqrt{s_{NN}} = 5.02$ TeV

Original

c+ production in Pb–Pb collisions at $\sqrt{s_{NN}} = 5.02$ TeV / Acharya, S; Adamova, D.; Adolfson, J; Aggarwal, M.; Rinella, G.; Agnello, M.; Agrawal, N; Bufalino, S.; Concas, M.; Grosa, F.; Ravasenga, I. - In: PHYSICS LETTERS. SECTION B. - ISSN 0370-2693. - STAMPA. - 793:(2019), pp. 212-223. [10.1016/j.physletb.2019.04.046]

Availability:

This version is available at: 11583/2848232 since: 2020-10-13T11:08:30Z

Publisher:

Elsevier B.V.

Published

DOI:10.1016/j.physletb.2019.04.046

Terms of use:

This article is made available under terms and conditions as specified in the corresponding bibliographic description in the repository

Publisher copyright

Elsevier postprint/Author's Accepted Manuscript

© 2019. This manuscript version is made available under the CC-BY-NC-ND 4.0 license
<http://creativecommons.org/licenses/by-nc-nd/4.0/>. The final authenticated version is available online at:
<http://dx.doi.org/10.1016/j.physletb.2019.04.046>

(Article begins on next page)



Λ_c^+ production in Pb–Pb collisions at $\sqrt{s_{NN}} = 5.02$ TeV

ALICE Collaboration*



ARTICLE INFO

Article history:

Received 12 October 2018

Received in revised form 26 March 2019

Accepted 17 April 2019

Available online 23 April 2019

Editor: L. Rolandi

ABSTRACT

A measurement of the production of prompt Λ_c^+ baryons in Pb–Pb collisions at $\sqrt{s_{NN}} = 5.02$ TeV with the ALICE detector at the LHC is reported. The Λ_c^+ and $\bar{\Lambda}_c^-$ were reconstructed at midrapidity ($|y| < 0.5$) via the hadronic decay channel $\Lambda_c^+ \rightarrow pK_S^0$ (and charge conjugate) in the transverse momentum and centrality intervals $6 < p_T < 12$ GeV/c and 0–80%. The Λ_c^+/D^0 ratio, which is sensitive to the charm quark hadronisation mechanisms in the medium, is measured and found to be larger than the ratio measured in minimum-bias pp collisions at $\sqrt{s} = 7$ TeV and in p–Pb collisions at $\sqrt{s_{NN}} = 5.02$ TeV. In particular, the values in p–Pb and Pb–Pb collisions differ by about two standard deviations of the combined statistical and systematic uncertainties in the common p_T interval covered by the measurements in the two collision systems. The Λ_c^+/D^0 ratio is also compared with model calculations including different implementations of charm quark hadronisation. The measured ratio is reproduced by models implementing a pure coalescence scenario, while adding a fragmentation contribution leads to an underestimation. The Λ_c^+ nuclear modification factor, R_{AA} , is also presented. The measured values of the R_{AA} of Λ_c^+ , D_s^+ and non-strange D mesons are compatible within the combined statistical and systematic uncertainties. They show, however, a hint of a hierarchy ($R_{AA}^{D^0} < R_{AA}^{D_s^+} < R_{AA}^{\Lambda_c^+}$), conceivable with a contribution from coalescence mechanisms to charm hadron formation in the medium.

© 2019 European Organization for Nuclear Research. Published by Elsevier B.V. This is an open access article under the CC BY license (<http://creativecommons.org/licenses/by/4.0/>). Funded by SCOAP³.

1. Introduction

Measurements of the production of open-heavy flavour hadrons in heavy-ion collisions provide important information on the properties of the Quark–Gluon Plasma (QGP), the state of strongly-interacting matter formed at the very high temperatures and energy densities reached in heavy-ion collisions [1,2]. Several measurements of the production and elliptic flow of D mesons and leptons from the decay of heavy-flavour hadrons in Pb–Pb collisions at the LHC and in Au–Au collisions at RHIC [3,4] indicate that charm quarks interact strongly with the medium constituents. In-medium energy loss is studied via the nuclear modification factor, R_{AA} , defined as the ratio of the yield in Pb–Pb collisions and that in pp collisions scaled by the number of binary nucleon–nucleon collisions. A model [5,6] including a significant fraction of low and intermediate transverse momentum (p_T) charm and beauty quarks hadronising via coalescence (or recombination) with light quarks from the medium better describes the experimental results. This mechanism is expected to also affect the production of D_s^+ given the strange-quark rich environment of the created medium. At higher transverse momentum ($p_T > 7$ GeV/c at LHC

energies [7]) hadronisation by vacuum fragmentation is expected to be the dominant production mechanism.

In this context, the study of charm baryons is essential to understand charm hadronisation. Models including coalescence predict an enhanced baryon-to-meson ratio at low and intermediate transverse momentum in comparison to that expected in pp collisions. This effect adds to the hadron-mass dependent transverse-momentum shift due to the presence of radial flow in heavy-ion collisions, that is able to explain the observed increase of the baryon-to-meson ratio in the light sector up to about 2 GeV/c [8]. The study of non-strange D-mesons, D_s^+ and Λ_c^+ could help to disentangle the role of coalescence and radial flow, because of the smaller mass differences than for light-flavour hadrons.

For the particular case of charm baryons, the possible existence of light di-quark bound states in the QGP could further enhance the Λ_c^+/D^0 ratio in the coalescence model [9]. An enhancement of the p_T -integrated Λ_c^+/D^0 ratio in the presence of a QGP is also predicted by the statistical hadronisation model [10], where at LHC energies the relative abundance of hadrons depends on their masses, their flavour content and the freeze-out temperature of the medium. In addition, an enhancement of charm-baryon production in Pb–Pb collisions would make the charm baryons an important fraction of the total charm production cross section.

The study of a potential enhancement effect in charm-baryon production in relativistic heavy-ion collisions requires a baseline

* E-mail address: alice-publications@cern.ch.

reference in smaller collision systems. The Λ_c^+ -baryon production was measured by the ALICE Collaboration in pp collisions at $\sqrt{s} = 7$ TeV in the transverse momentum and rapidity (y) intervals $1 < p_T < 8$ GeV/c and $|y| < 0.5$ [11]. The obtained baryon-to-meson ratio is larger than previous measurements at lower centre-of-mass energies and in different collision systems (see Ref. [11] and references therein), and also higher than the results reported by the LHCb Collaboration in pp collisions at $\sqrt{s} = 7$ TeV in the rapidity range $2.0 < y < 4.5$ [12]. Expectations from perturbative Quantum Chromodynamics (pQCD) calculations and Monte Carlo event generators underpredict the data, indicating that the fragmentation of charm quarks is not fully understood [11] and partially challenged by data collected so far at the LHC, as discussed extensively in Ref. [13]. The production of Λ_c^+ baryons was also measured by the ALICE Collaboration in p-Pb collisions at $\sqrt{s_{NN}} = 5.02$ TeV in $2 < p_T < 12$ GeV/c and $-0.96 < y < 0.04$ [11], and a measurement in the same collision system by the LHCb Collaboration [14] is also available. The Λ_c^+ nuclear modification factor R_{pPb} is compatible with unity within statistical and systematic uncertainties. The baryon-to-meson ratios Λ_c^+/D^0 measured in pp and p-Pb collisions are compatible within uncertainties. A model [15,16] including hadronisation via coalescence in these collision systems has been proposed to describe the measurements at LHC energies.

This letter reports measurements of the production of the prompt charm baryon Λ_c^+ and its charge conjugate in Pb-Pb collisions at $\sqrt{s_{NN}} = 5.02$ TeV with the ALICE detector [17] at the LHC. Hereafter, Λ_c refers indistinctly to both particle and anti-particle, and all mentioned decay channels refer also to their charge conjugates. The Λ_c^+ corrected yield is obtained as the average of the particle and the anti-particle yield. The notation Λ_c^+ is used when referring to this average, and thus to indicate physics quantities such as the Λ_c^+/D^0 ratio. The measurement was performed in the 0–80% centrality class in the transverse momentum and rapidity intervals $6 < p_T < 12$ GeV/c and $|y| < 0.5$. Only prompt Λ_c -baryons were considered: the beauty-hadron feed-down was subtracted, as described in the next section. The D^0 -meson yield was obtained in the same transverse momentum and centrality interval as the Λ_c -baryon, following the analysis procedure described in Ref. [18].

2. Data sample and analysis strategy

The measurement of the Λ_c -baryon production was performed by reconstructing the decays $\Lambda_c^+ \rightarrow pK_S^0$ with a branching ratio (BR) equal to $(1.58 \pm 0.08)\%$ and $K_S^0 \rightarrow \pi^+\pi^-$ with BR = $(69.20 \pm 0.05)\%$ [19]. The D^0 mesons were reconstructed in the decay channel $D^0 \rightarrow K^-\pi^+$ with BR = $(3.93 \pm 0.04)\%$ [19]. The Λ_c and D^0 candidates were reconstructed in the same transverse momentum, rapidity and centrality intervals. The analysis benefits from the tracking and particle identification capabilities of the ALICE central barrel detectors located within a large solenoidal magnet that provides a magnetic field of 0.5 T parallel to the LHC beam axis. A complete description of the ALICE apparatus and its performance can be found in Refs. [17,20]. The main detectors used in this analysis include the Inner Tracking System (ITS) [21], the Time Projection Chamber (TPC) [22], the Time-Of-Flight detector (TOF) [23] and the V0 detector [24] located inside the solenoidal magnet, as well as the Zero Degree Calorimeters (ZDC) [17] located in the LHC tunnel at about ± 112.5 m from the nominal interaction point and composed of two proton and two neutron calorimeters.

The analysed data sample consists of about 83×10^6 Pb-Pb collisions at $\sqrt{s_{NN}} = 5.02$ TeV, corresponding to an integrated luminosity of $\mathcal{L}_{int} \approx 13.4 \mu\text{b}^{-1}$. The interaction trigger was provided

by the coincident signals from the two arrays of the V0 detector, covering the pseudorapidity intervals $-3.7 < \eta < -1.7$ and $2.8 < \eta < 5.1$. Background events from beam-gas interactions were removed in the offline analysis using the timing information provided by the V0 and the neutron ZDC. Only events with a primary vertex reconstructed within ± 10 cm from the centre of the detector along the beam line were considered for the analysis. Events were selected in the centrality class 0–80%, defined in terms of percentiles of the hadronic Pb-Pb cross section, using the amplitudes of the signals in the V0 arrays [25].

The Λ_c candidates were constructed by combining a proton candidate track with a K_S^0 candidate identified through its V-shaped neutral decay topology (V^0). The charged tracks and the K_S^0 candidates were selected as described in Ref. [11] for pp collisions with additional requirements to reduce the larger combinatorial background due to the higher charged-track multiplicity in Pb-Pb with respect to pp collisions. In particular, candidate proton tracks were required to have a hit in the innermost ITS layer and tighter selections on the K_S^0 were applied: a maximum distance of closest approach between the V^0 decay tracks of 0.4 cm, a minimum cosine of the V^0 pointing angle to the primary vertex of 0.9998, a minimum p_T of the K_S^0 candidates of 1 GeV/c, and a cut in the Armenteros-Podolanski space [26] to remove contributions from Λ decays. The identification of protons was based on the specific ionisation energy loss dE/dx in the TPC and on the time of flight measured with the TOF detector, using as a discriminating variable (n_σ) the difference between the measured value and the expected value for the proton mass hypothesis divided by the detector resolution. A $|n_\sigma| < 3$ selection was applied on the TPC dE/dx and TOF time-of-flight measurements for tracks with $p_T < 3$ GeV/c. For tracks with $p_T > 3$ GeV/c an asymmetric selection was used to limit the contamination from pions in the TPC and from kaons in the TOF and the requirements were $-3 < n_\sigma^{\text{TPC}} < 2$ and $-2 < n_\sigma^{\text{TOF}} < 3$ for the TPC and TOF signals. Tracks without TOF information were discarded. The Λ_c candidates were selected requiring a cosine of the proton emission angle in the Λ_c centre-of-mass system with respect to the Λ_c momentum direction smaller than 0.5. A selection on the signed transverse impact parameter of the proton, i.e. the distance of closest approach between the proton track and the primary vertex, larger than 0.003 cm was also applied (the sign of the impact parameter is defined as positive when the angle between the Λ_c flight line and the momentum vector is smaller than 90°).

The D^0 candidates were reconstructed by combining pairs of tracks with the proper charge sign combination and selected in the interval $6 < p_T < 12$ GeV/c using the same criteria described in Ref. [18] for the interval $6 < p_T < 7$ GeV/c in the 10% most central Pb-Pb collisions.

After all selections, the acceptance in rapidity for Λ_c and D^0 candidates drops steeply to zero for $|y| > 0.8$ in the p_T interval used for the analysis. Therefore, a fiducial acceptance cut $|y| < 0.8$ was applied as described in Refs. [11] and [18].

The Λ_c and D^0 raw yields were extracted by fitting the invariant mass distributions of the candidates passing the selection criteria. The fit functions consist of a Gaussian to describe the signal and an exponential to describe the background. In the case of the Λ_c , the width of the Gaussian was fixed to the value obtained from Monte Carlo simulations. The stability of the Λ_c signal extraction was verified by fitting the invariant mass distribution after the subtraction of the background evaluated with an event-mixing technique and no discrepancy between the two approaches was observed. For the D^0 -meson yield, the contribution of signal candidates with the wrong $K-\pi$ mass assignment (reflections) to the invariant-mass distribution was taken into account by including an additional term, parameterised from simulations with a double-Gaussian shape, in the fit function [27].

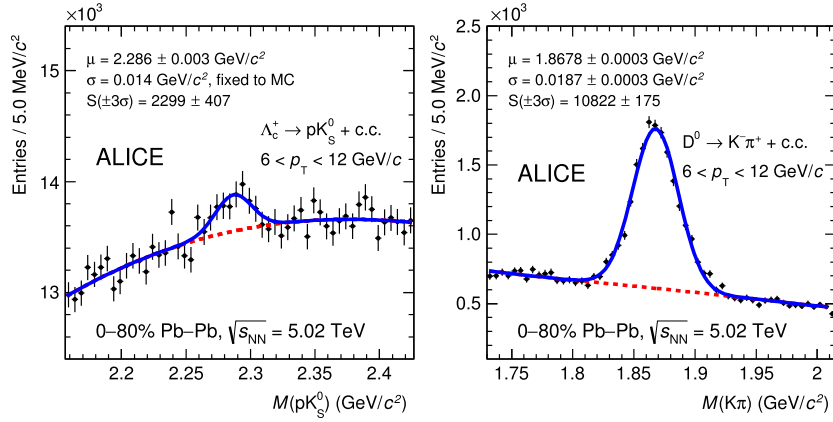


Fig. 1. Invariant-mass distributions for the Λ_c (left) and D^0 (right) candidates in the momentum interval $6 < p_T < 12$ GeV/c and for the 0–80% centrality class. The dashed curves represent the fit to the background, while the solid curves represent the total fit function.

The invariant mass distributions of the selected Λ_c and D^0 candidates are shown in Fig. 1.

The prompt Λ_c^+ (D^0) production yield was calculated as

$$\left. \frac{dN_{\text{prompt}}^{\Lambda_c^+ (D^0)}}{dp_T} \right|_{|y| < 0.5} = \frac{1}{2} \frac{1}{c_{\Delta y}} \frac{1}{\Delta p_T} \frac{f_{\text{prompt}} \cdot N_{\text{raw}}|_{|y| < 0.8}}{(\text{Acc} \times \varepsilon)_{\text{prompt}} \cdot \text{BR} \cdot N_{\text{evt}}}, \quad (1)$$

where N_{raw} is the raw yield (sum of particles and anti-particles) in the transverse momentum interval of width Δp_T , f_{prompt} is the fraction of prompt Λ_c (D^0) in the raw yield, $(\text{Acc} \times \varepsilon)$ is the product of acceptance and reconstruction efficiency for prompt Λ_c (D^0), BR is the branching ratio of the considered decay mode and N_{evt} is the number of events considered for the analysis. The correction factor for the rapidity coverage $c_{\Delta y}$ was computed as the ratio of the generated Λ_c (D^0) yield in $|y| < 0.8$ and that in $|y| < 0.5$. The factor 1/2 takes into account that the raw yield is the sum of particles and anti-particles, while the production yield is reported as their average.

The correction for the detector acceptance and reconstruction efficiency was determined by means of Monte Carlo (MC) simulations. The underlying Pb–Pb events at $\sqrt{s_{\text{NN}}} = 5.02$ TeV were simulated using the HIJING v1.383 [28] generator and prompt and feed-down Λ_c (D^0) were added using the PYTHIA v6.421 [29] generator with Perugia 11 tune. The generated particles were transported through the ALICE detector using the GEANT3 [30] package. A realistic detector response was introduced in the simulations to reproduce the performance of the ALICE detector system during data taking.

The p_T distributions of the Λ_c and D^0 in PYTHIA were corrected in order to obtain more realistic distributions. The same p_T -dependent weighting factor, calculated as the ratio of the measured D^0 p_T distribution in finer p_T bins [18] and the one simulated with PYTHIA, was used for both particles. The Λ_c and D^0 reconstruction efficiency in the large centrality class 0–80% was obtained as the weighted average of the efficiencies in smaller centrality classes to take into account the variation of the efficiency and the scaling of the yields of the Λ_c baryons and D^0 mesons with centrality. The applied weights were calculated as the product of the R_{AA} of the D^0 and the average number of nucleon–nucleon collisions ($\langle N_{\text{coll}} \rangle$) in the centrality class considered [18]. The $(\text{Acc} \times \varepsilon)$ value is about 6% for prompt and about 9% for feed-down Λ_c and about 8% for prompt and about 11% for feed-down D^0 .

The prompt Λ_c (D^0) fraction, f_{prompt} , was calculated as

$$\begin{aligned} f_{\text{prompt}} &= 1 - \left(\frac{N_{\text{feed-down}}^{\Lambda_c (D^0)}}{N_{\text{prompt}}^{\Lambda_c (D^0)}} \right) = \\ &= 1 - \langle T_{\text{AA}} \rangle \cdot \left. \frac{d^2\sigma}{dy dp_T} \right|_{\text{feed-down}}^{\text{FONLL}} \cdot R_{\text{AA}}^{\text{feed-down}} \cdot \frac{(\text{Acc} \times \varepsilon)_{\text{feed-down}} \cdot c_{\Delta y} \cdot \Delta p_T \cdot \text{BR} \cdot N_{\text{evt}}}{N_{\text{raw}}/2}. \end{aligned} \quad (2)$$

The contribution of Λ_c (D^0) from beauty-hadron decays was estimated using the FONLL [31,32] beauty-production cross sections as described in detail in Ref. [33]. The fraction of beauty quarks that fragment to beauty hadrons and subsequently decay into Λ_c baryons $f(b \rightarrow \Lambda_c) = 0.073$ was taken from Ref. [34]. The beauty-hadron decay kinematics were modeled using the EVTGEN [35] package. The $(\text{Acc} \times \varepsilon)_{\text{feed-down}}$ term for both particles was calculated from the Monte Carlo simulations described above. The average nuclear overlap function, $\langle T_{\text{AA}} \rangle$, was estimated via Glauber model calculations [36,37]. In this formalism the nuclear modification factor R_{AA} is then the ratio of the yield in Pb–Pb collisions and the production cross section in pp collisions scaled by $\langle T_{\text{AA}} \rangle$.

A hypothesis on the $R_{\text{AA}}^{\text{feed-down}}$ of feed-down Λ_c and D^0 is used. For the D^0 , the hypothesis is the same as in other analyses (e.g. in Ref. [18]): the central value is obtained by assuming $R_{\text{AA}}^{\text{feed-down } D^0} / R_{\text{AA}}^{\text{prompt } D^0} = 2$, justified by the CMS measurement of J/ψ from B-meson decays [38] and by the ALICE and CMS measurements of D mesons [18,39] indicating that prompt charm mesons are more suppressed than non-prompt charm mesons. The ratio is varied in the interval $1 < R_{\text{AA}}^{\text{feed-down } D^0} / R_{\text{AA}}^{\text{prompt } D^0} < 3$ to estimate the systematic uncertainty. Since no measurements of beauty-baryon production in nucleus–nucleus collisions are available, for the Λ_c the central hypothesis was taken from model calculations which predict $R_{\text{AA}}^{\text{feed-down } \Lambda_c^+} / R_{\text{AA}}^{\text{prompt } \Lambda_c^+} = 2$ when considering c and b quark fragmentation and energy loss in the medium [40]. The ratio $R_{\text{AA}}^{\text{feed-down } \Lambda_c^+} / R_{\text{AA}}^{\text{prompt } \Lambda_c^+}$ was decomposed into two terms to estimate the uncertainty on the assumption:

$$\frac{R_{\text{AA}}^{\text{feed-down } \Lambda_c^+}}{R_{\text{AA}}^{\text{prompt } \Lambda_c^+}} = \frac{R_{\text{AA}}^{\text{feed-down } D^0}}{R_{\text{AA}}^{\text{prompt } D^0}} \cdot \frac{(\Lambda_c^+ / D^0)_{\text{PbPb, feed-down}}}{(\Lambda_c^+ / D^0)_{\text{pp, feed-down}}} \cdot \frac{(\Lambda_c^+ / D^0)_{\text{PbPb, prompt}}}{(\Lambda_c^+ / D^0)_{\text{pp, prompt}}}. \quad (3)$$

The first term is the same as for the D^0 and thus the same hypothesis is adopted. The second term is varied in the range 0.5–1.5

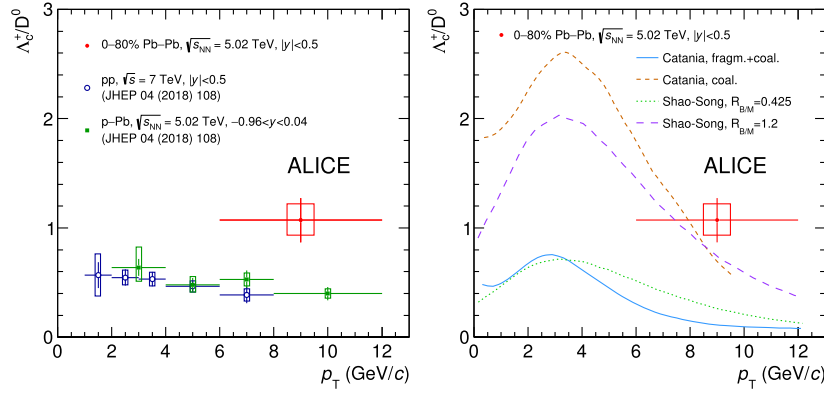


Fig. 2. Λ_c^+/D^0 ratio as a function of p_T in 0–80% most central Pb–Pb collisions compared with the measurements in pp and p–Pb collisions [11] (left), and model calculations [7] (right). Statistical and systematic uncertainties are presented as vertical bars and boxes, respectively.

Table 1

Systematic uncertainties on the corrected yields. When the uncertainty was found to be $< 1\%$, it was considered negligible (negl. in the table).

Uncertainty	Λ_c^+	D^0
Raw-yield extraction	8%	2%
Tracking efficiency	3.6%	5%
PID	5%	negl.
Cut variation	2%	5%
MC p_T shape	2%	negl.
MC centrality weights	3%	negl.
Feed-down subtraction	+6% –12%	+12% –13%
Branching ratio	5%	1%

to calculate the systematic uncertainty. The upper limit is determined a-posteriori such that $R_{AA}^{\text{feed-down}} \Lambda_c^+ < 2$ as suggested by the fact that no baryon R_{AA} exceeds this value. The uncertainties on the two terms are added in quadrature. The resulting values of f_{prompt} are about 0.93 and 0.81 for the Λ_c and D^0 , respectively.

A summary of the systematic uncertainties on the corrected Λ_c^+ and D^0 yields is shown in Table 1. The D^0 systematic uncertainties on the particle identification (PID), tracking and cut variation are taken from Ref. [18] and are not discussed in the following.

The systematic uncertainty on the raw-yield extraction for Λ_c and D^0 was estimated by repeating the fits several times varying (i) the lower and upper limits of the fit range, (ii) the background fit function and (iii) only in the case of the Λ_c , considering the Gaussian mean and width as free parameters in the fit. In addition, the signal yield was obtained by integrating the invariant-mass distribution after subtracting the background estimated from a fit to the sidebands.

For the Λ_c , the systematic uncertainty on the tracking efficiency was evaluated by comparing the probability of matching tracks reconstructed in the TPC to ITS hits in data and simulation and by varying the quality cuts to select the tracks used in the analysis. The contribution due to the variation of the quality cuts was evaluated using protons from Λ decays and an inclusive K_S^0 sample and by calculating the ratio of the corrected yields obtained using different selection criteria. The uncertainty on the ITS-TPC matching efficiency is defined as the relative difference of the matching efficiency in data and simulations after weighting the relative abundances of primary and secondary particles in the simulations to match those in data. The latter were estimated via fits to the track impact-parameter distributions. The values calculated as a function of track momentum were propagated to the p_T -differential uncertainty of the Λ_c using a Monte Carlo simulation. A 3% systematic uncertainty on the ITS-TPC matching efficiency of proton

tracks was assigned while for the K_S^0 the matching is not required. The uncertainty resulting from these studies was added in quadrature to the uncertainty on the track selection.

The systematic uncertainty on the Λ_c PID efficiency was evaluated using protons from the decay of Λ baryons. The ratio of the Λ yield measured with PID to that measured without PID was calculated in both data and MC and their difference was used to estimate the systematic uncertainty.

Systematic uncertainties on the efficiencies can also arise from possible differences in the distributions and resolutions of selection variables between data and simulation. The systematic effect induced by these imperfections was estimated by repeating the analysis varying the main selection criteria for the candidates. The efficiencies determined from the simulations depend also on the generated p_T distributions of the Λ_c and the D^0 . The central values of the correction factors were obtained by re-weighting the Λ_c and D^0 distributions generated by PYTHIA as described above. For the D^0 , the efficiencies calculated with and without the p_T weights are compatible and therefore no uncertainty was assigned. For the Λ_c , the systematic uncertainty was defined by considering the variation of the efficiencies determined with different generated p_T shapes. The new Λ_c p_T shape was calculated by multiplying the measured D^0 p_T distribution with the Λ_c^+/D^0 ratios predicted by the models [6] and [41].

Finally, the efficiencies in the centrality class 0–80% depend on the centrality weights used to combine the efficiencies in the smaller centrality classes. The stability of the efficiencies against the variation of the centrality weights was tested by recalculating the efficiencies without weighting for $\langle N_{\text{coll}} \rangle$ and, for the Λ_c , using as an alternative centrality weight the product $\Lambda/K_S^0 \cdot \langle N_{\text{coll}} \rangle$, where the ratio Λ/K_S^0 is taken from Ref. [8].

The systematic uncertainty on the subtraction of feed-down from beauty-hadron decays was estimated by varying (i) the p_T -differential cross section of feed-down Λ_c (D^0) from FONLL calculations within the theoretical uncertainties (see Ref. [11] for details on the Λ_c and Ref. [33] for the D^0) and (ii) the ratio of prompt and feed-down R_{AA} as described above.

The production yields of Λ_c and D^0 also have a global systematic uncertainty due to the branching ratio.

3. Results

The yield of prompt Λ_c^+ baryons measured in Pb–Pb collisions at $\sqrt{s_{NN}} = 5.02$ TeV in the 0–80% centrality class in $|y| < 0.5$ and $6 < p_T < 12$ GeV/c is $N^{\Lambda_c^+} = (2.1 \pm 0.4 \text{ (stat.)}_{-0.4}^{+0.3} \text{ (syst.)}) \times 10^{-2}$.

The measured Λ_c^+/D^0 ratio is shown in Fig. 2. The systematic uncertainty of the Λ_c^+ -baryon production arising from the track-

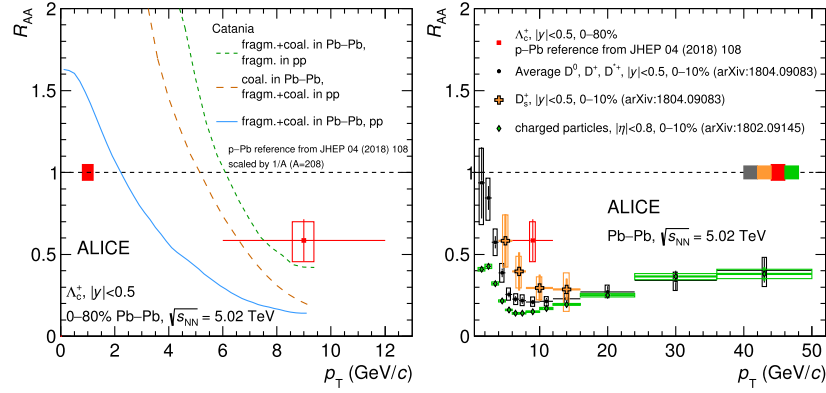


Fig. 3. R_{AA} of prompt Λ_c^+ compared with model calculations [7,15,16] (left), and the non-strange D mesons, D_s^+ , and charged particle R_{AA} in 0–10% most central Pb–Pb collisions for $p_T > 1$ GeV/c [18,42] (right). Statistical, systematic and normalisation uncertainties are presented as vertical bars, empty boxes and shaded boxes around unity, respectively.

ing efficiency was treated as fully correlated to that of the D^0 meson. The contribution to the feed-down uncertainty related to heavy-quark energy loss and that originating from the FONLL uncertainty on the feed-down Λ_c^+ and D^0 cross sections were treated as fully correlated when propagated to the ratio. All the other sources of uncertainty were considered as uncorrelated. In the left panel of Fig. 2, the Λ_c^+/D^0 ratio measured in Pb–Pb collisions is compared with the results obtained by the ALICE Collaboration in minimum-bias pp and p–Pb collisions at $\sqrt{s} = 7$ TeV and $\sqrt{s_{NN}} = 5.02$ TeV [11], respectively. The ratio measured in Pb–Pb collisions is higher than that measured in pp and p–Pb collisions. In particular, the values in p–Pb and Pb–Pb collisions differ by about two standard deviations of the combined statistical and systematic uncertainties in $6 < p_T < 12$ GeV/c.

The Λ_c^+/D^0 ratio in Pb–Pb collisions is compared with theoretical model calculations in the right panel of Fig. 2. The Catania model [7] provides two different treatments of hadronisation. In one case, charm quarks hadronise via coalescence only. In the other case, a coalescence plus vacuum fragmentation modelling of hadronisation is considered: at increasing p_T the coalescence probability decreases and eventually vacuum fragmentation takes over. For D^0 mesons, the shape of the fragmentation function is tuned assuring that the experimental results on D-meson production in pp collisions are well described by a fragmentation hadronisation mechanism. Data from e^+e^- collisions are used to fix the shape of the fragmentation functions for Λ_c^+ . The coalescence mechanism is treated as a three-quark process and implemented through the Wigner formalism. The momentum spectrum of hadrons formed by coalescence is obtained from the quark phase-space distributions and the hadron wave function. The width parameters of the hadron wave functions are calculated from the charge radius of the hadrons according to the quark model. The hadron wave function normalisation is determined by requiring a total coalescence probability for charm quarks equal to unity for zero-momentum heavy quarks. Moreover, the contributions from the first excited states for D and Λ_c hadrons were included in the calculations. The experimental results are described by the model calculation including coalescence only. The curve obtained by modelling charm hadronisation via vacuum fragmentation plus coalescence, which describes the Λ_c^+/D^0 ratio measured in Au–Au collisions at RHIC energy [43], significantly underestimates the measurement in Pb–Pb collisions at the LHC. In the Shao-Song model [15,16], coalescence involves quarks which are close in momentum space, and it takes place mainly for the quark with a given fraction of the momentum of the hadron. It does not consider the Wigner formalism to describe the spatial and momentum distribution of quarks in a hadron. It can not directly predict the absolute magnitude of the Λ_c^+/D^0 ra-

tio because the relative production of single-charm baryons and single-charm mesons R_{BM} is treated as a parameter of the model. The curve obtained by considering $R_{BM} = 0.425$, which is the value needed to describe the results in pp and p–Pb collisions, underestimates the Λ_c^+/D^0 ratio measured in Pb–Pb collisions. An $R_{BM} = 1.2$ is needed to achieve a better description of the experimental results in Pb–Pb collisions. However, the hadronisation mechanism via quark coalescence included in the model is responsible of the p_T dependence of the Λ_c^+/D^0 ratio, which needs to be verified by comparing to a measurement at lower p_T . The R_{AA} of prompt Λ_c^+ was obtained by considering as reference the Λ_c^+ cross section measured in p–Pb collisions at $\sqrt{s_{NN}} = 5.02$ TeV [11] scaled by $1/A$ ($A = 208$) and corrected for the different rapidity coverage of the p–Pb measurement. The cross section measured in p–Pb was scaled in each p_T interval to $|y| < 0.5$ using a correction factor obtained with FONLL calculations [31,32]. The correction factor was determined from the ratios of the cross sections calculated with FONLL in the rapidity intervals $|y| < 0.5$ and $-0.96 < y < 0.04$. Since FONLL does not provide predictions for Λ_c^+ baryons, the average of the correction factors obtained for D^0 , D^+ and bare charm quarks, which was found to be 1.024 ± 0.008 , was used. The choice of using the p–Pb cross section to obtain the reference for the R_{AA} was motivated by the fact that it was measured up to $p_T = 12$ GeV/c, while the measurement in pp collisions at $\sqrt{s} = 7$ TeV in $|y| < 0.5$ only reaches $p_T = 8$ GeV/c. In addition, the Λ_c^+ nuclear modification factor measured in p–Pb collisions is consistent with unity for $p_T > 2$ GeV/c [11]. The Λ_c^+ reference cross section in $6 < p_T < 12$ GeV/c was obtained by combining the results in the transverse momentum intervals $6 < p_T < 8$ GeV/c and $8 < p_T < 12$ GeV/c. The uncertainties were propagated treating the statistical and the systematic uncertainties on the yield extraction as uncorrelated and the other sources of systematic uncertainty as correlated in p_T . The Λ_c^+ R_{AA} also has a 3.75% uncertainty due to the normalisation of the Λ_c^+ p–Pb cross section at $\sqrt{s_{NN}} = 5.02$ TeV [11] and a 2.4% uncertainty on the average nuclear overlap function $\langle T_{AA} \rangle$, which were added in quadrature. In the left panel of Fig. 3, the R_{AA} of prompt Λ_c^+ is compared with Catania model calculations [7]. The three curves are obtained by considering different treatments of the hadronisation mechanisms in pp and Pb–Pb collisions. The short-dashed curve represents the Λ_c^+ R_{AA} as obtained by including both vacuum fragmentation and quark coalescence for charm hadronisation in Pb–Pb and only fragmentation in pp collisions. The long-dashed curve includes only coalescence in Pb–Pb and fragmentation plus coalescence in pp collisions. The solid curve is obtained by considering fragmentation plus coalescence in both collision systems. The limited precision and the large p_T interval of this first measurement prevent us to

draw a firm conclusion on which combination of the hadronisation mechanisms in the two collision systems better describes the result. Moreover, the comparison between the different scenarios obtained from the Catania model demonstrates that it is crucial to also understand the Λ_c^+ production mechanism in pp collisions to interpret the R_{AA} measurement. The right panel of Fig. 3 shows the R_{AA} of prompt Λ_c^+ baryons measured in the 0–80% centrality class (that is dominated by the 0–10% production given the scaling of the yields with $N_{coll} \cdot R_{AA}$) compared with the average nuclear modification factors of non-strange D mesons, D_s^+ mesons, and charged particles measured in the 0–10% centrality class [18]. The R_{AA} of charged particles is smaller than that of D mesons by more than 2σ of the combined statistical and systematic uncertainties up to $p_T = 8$ GeV/c, while they are compatible within 1σ for $p_T > 10$ GeV/c. The R_{AA} values of D_s^+ mesons are larger than those of non-strange D mesons, but the two measurements are compatible within one standard deviation of the combined uncertainties [18]. A hint of a larger Λ_c^+ R_{AA} with respect to non-strange D mesons is observed, although the results are compared for different centrality classes. A D^0 $R_{AA} = 0.27 \pm 0.01(\text{stat.}) \pm 0.04(\text{syst.})$ was measured in $6 < p_T < 12$ GeV/c in the 0–80% centrality class. The D^0 R_{AA} has also a 3.5% uncertainty arising from the normalisation of the cross section measured in pp collisions at $\sqrt{s} = 7$ TeV, and a 2.4% uncertainty on the average nuclear overlap function $\langle T_{AA} \rangle$. The p_T -differential cross section of prompt D^0 mesons with $|y| < 0.5$ in pp collisions at $\sqrt{s} = 5.02$ TeV, used as reference for the nuclear modification factor, was obtained by scaling the measurement at $\sqrt{s} = 7$ TeV [44] to $\sqrt{s} = 5.02$ TeV using FONLL calculations [31,32]. The scaling was applied to the D^0 cross section obtained in $6 < p_T < 12$ GeV/c by combining the results in the p_T intervals of the measurement at $\sqrt{s} = 7$ TeV. The statistical and the systematic uncertainties on the yield extraction were propagated as uncorrelated. The other contributions to the systematic uncertainty were considered as fully correlated among the p_T intervals. A difference of about 1.7σ is obtained when comparing the Λ_c^+ R_{AA} with that of the D^0 in $6 < p_T < 12$ GeV/c and 0–80% centrality interval. This observation is qualitatively in agreement with a scenario where a significant fraction of charm quarks hadronise via coalescence with light quarks from the medium leading to an enhanced baryon production with respect to that of mesons.

4. Summary

The measurement of the production of prompt Λ_c^+ baryons in the 0–80% most central Pb–Pb collisions at $\sqrt{s_{NN}} = 5.02$ TeV was presented. The result was obtained at midrapidity, $|y| < 0.5$, in the $6 < p_T < 12$ GeV/c transverse momentum interval. The Λ_c^+/D^0 ratio is larger than the ratio measured in pp and p–Pb collisions at $\sqrt{s} = 7$ TeV and $\sqrt{s_{NN}} = 5.02$ TeV [11], respectively. The Λ_c^+/D^0 ratio measured in Pb–Pb collisions is described by a model calculation implementing only charm quark hadronisation via quark coalescence and it is underestimated when also vacuum fragmentation is included. The comparison of the Λ_c^+ nuclear modification factor with non-strange D and D_s^+ meson results, which were measured in 0–10% most central Pb–Pb collisions, suggests a hint of a hierarchy, conceivable in a scenario where charm quark hadronisation can occur via coalescence processes, thus enhancing the Λ_c^+ -baryon and D_s^+ -meson production with respect to non-strange D mesons. However, the limited precision of this first measurement prevents us from drawing a firm conclusion.

A higher precision for a Λ_c^+ -baryon production measurement with finer granularity in p_T and centrality will be achieved with future datasets to be collected during LHC Run 2 and, in particular,

during the LHC Run 3 and 4, following the major upgrade of the ALICE apparatus [45,46].

Acknowledgements

The ALICE Collaboration would like to thank all its engineers and technicians for their invaluable contributions to the construction of the experiment and the CERN accelerator teams for the outstanding performance of the LHC complex. The ALICE Collaboration gratefully acknowledges the resources and support provided by all Grid centres and the Worldwide LHC Computing Grid (WLCG) collaboration. The ALICE Collaboration acknowledges the following funding agencies for their support in building and running the ALICE detector: A. I. Alikhanyan National Science Laboratory (Yerevan Physics Institute) Foundation (ANSL), State Committee of Science and World Federation of Scientists (WFS), Armenia; Austrian Academy of Sciences and Nationalstiftung für Forschung, Technologie und Entwicklung, Austria; Ministry of Communications and High Technologies, National Nuclear Research Center, Azerbaijan; Conselho Nacional de Desenvolvimento Científico e Tecnológico (CNPq), Universidade Federal do Rio Grande do Sul (UFRGS), Financiadora de Estudos e Projetos (Finep) and Fundação de Amparo à Pesquisa do Estado de São Paulo (FAPESP), Brazil; Ministry of Science & Technology of China (MSTC), National Natural Science Foundation of China (NSFC) and Ministry of Education of China (MOEC), China; Ministry of Science and Education, Croatia; Centro de Aplicaciones Tecnológicas y Desarrollo Nuclear (CEADEN), Cubaenergía, Cuba; Ministry of Education, Youth and Sports of the Czech Republic, Czech Republic; The Danish Council for Independent Research | Natural Sciences, the Carlsberg Foundation and Danish National Research Foundation (DNRF), Denmark; Helsinki Institute of Physics (HIP), Finland; Commissariat à l’Energie Atomique (CEA) and Institut National de Physique Nucléaire et de Physique des Particules (IN2P3) and Centre National de la Recherche Scientifique (CNRS), France; Bundesministerium für Bildung, Wissenschaft, Forschung und Technologie (BMBF) and GSI Helmholtzzentrum für Schwerionenforschung GmbH, Germany; General Secretariat for Research and Technology, Ministry of Education, Research and Religions, Greece; National Research, Development and Innovation Office, Hungary; Department of Atomic Energy Government of India (DAE), Department of Science and Technology, Government of India (DST), University Grants Commission, Government of India (UGC) and Council of Scientific and Industrial Research (CSIR), India; Indonesian Institute of Science, Indonesia; Centro Fermi - Museo Storico della Fisica e Centro Studi e Ricerche Enrico Fermi and Istituto Nazionale di Fisica Nucleare (INFN), Italy; Institute for Innovative Science and Technology, Nagasaki Institute of Applied Science (IIST), Japan Society for the Promotion of Science (JSPS) KAKENHI and Japanese Ministry of Education, Culture, Sports, Science and Technology (MEXT), Japan; Consejo Nacional de Ciencia (CONACYT) y Tecnología, through Fondo de Cooperación Internacional en Ciencia y Tecnología (FONCICYT) and Dirección General de Asuntos del Personal Académico (DGAPA), Mexico; Nederlandse Organisatie voor Wetenschappelijk Onderzoek (NWO), Netherlands; The Research Council of Norway, Norway; Commission on Science and Technology for Sustainable Development in the South (COMSATS), Pakistan; Pontificia Universidad Católica del Perú, Peru; Ministry of Science and Higher Education and National Science Centre, Poland; Korea Institute of Science and Technology Information and National Research Foundation of Korea (NRF), Republic of Korea; Ministry of Education and Scientific Research, Institute of Atomic Physics and Romanian National Agency for Science, Technology and Innovation, Romania; Joint Institute for Nuclear Research (JINR), Ministry of Education and Science of the Russian Federation and National Research Centre Kurchatov Institute, Russia; Ministry of

Education, Science, Research and Sport of the Slovak Republic, Slovakia; National Research Foundation of South Africa, South Africa; Swedish Research Council (VR) and Knut & Alice Wallenberg Foundation (KAW), Sweden; European Organization for Nuclear Research, Switzerland; National Science and Technology Development Agency (NSDTA), Suranaree University of Technology (SUT) and Office of the Higher Education Commission under NRU project of Thailand, Thailand; Turkish Atomic Energy Agency (TAEK), Turkey; National Academy of Sciences of Ukraine, Ukraine; Science and Technology Facilities Council (STFC), United Kingdom; National Science Foundation of the United States of America (NSF) and United States Department of Energy, Office of Nuclear Physics (DOE NP), United States of America.

References

- [1] P. Braun-Munzinger, V. Koch, T. Schaefer, J. Stachel, Properties of hot and dense matter from relativistic heavy ion collisions, *Phys. Rep.* 621 (2016) 76–126, arXiv:1510.00442 [nucl-th].
- [2] A. Bazavov, et al., Equation of state in (2+1)-flavor QCD, *Phys. Rev. D* 90 (2014) 094503, <https://link.aps.org/doi/10.1103/PhysRevD.90.094503>.
- [3] A. Andronic, et al., Heavy-flavour and quarkonium production in the LHC era: from proton–proton to heavy-ion collisions, *Eur. Phys. J. C* 76 (3) (2016) 107, arXiv:1506.03981 [nucl-ex].
- [4] F. Prino, R. Rapp, Open heavy flavor in QCD matter and in nuclear collisions, *J. Phys. G* 43 (9) (2016) 093002, arXiv:1603.00529 [nucl-ex].
- [5] V. Greco, C.M. Ko, R. Rapp, Quark coalescence for charmed mesons in ultrarelativistic heavy ion collisions, *Phys. Lett. B* 595 (2004) 202–208, arXiv:nucl-th/0312100 [nucl-th].
- [6] Y. Oh, C.M. Ko, S.H. Lee, S. Yasui, Heavy baryon/meson ratios in relativistic heavy ion collisions, *Phys. Rev. C* 79 (2009) 044905, arXiv:0901.1382 [nucl-th].
- [7] S. Plumari, V. Minissale, S.K. Das, G. Coci, V. Greco, Charmed hadrons from coalescence plus fragmentation in relativistic nucleus–nucleus collisions at RHIC and LHC, *Eur. Phys. J. C* 78 (4) (2018) 348, arXiv:1712.00730 [hep-ph].
- [8] ALICE Collaboration, B. Abelev, et al., K_S^0 and Λ production in Pb–Pb collisions at $\sqrt{s_{NN}} = 2.76$ TeV, *Phys. Rev. Lett.* 111 (2013) 222301, arXiv:1307.5530 [nucl-ex].
- [9] S.H. Lee, K. Ohnishi, S. Yasui, I.-K. Yoo, C.-M. Ko, Λ_c enhancement from strongly coupled quark–gluon plasma, *Phys. Rev. Lett.* 100 (2008) 222301, arXiv:0709.3637 [nucl-th].
- [10] I. Kuznetsova, J. Rafelski, Heavy flavor hadrons in statistical hadronization of strangeness-rich QGP, *Eur. Phys. J. C* 51 (2007) 113–133, arXiv:hep-ph/0607203 [hep-ph].
- [11] ALICE Collaboration, S. Acharya, et al., Λ_c^+ production in pp collisions at $\sqrt{s} = 7$ TeV and in p–Pb collisions at $\sqrt{s_{NN}} = 5.02$ TeV, *J. High Energy Phys.* 04 (2018) 108, arXiv:1712.09581 [nucl-ex].
- [12] LHCb Collaboration, R. Aaij, et al., Prompt charm production in pp collisions at $\sqrt{s} = 7$ TeV, *Nucl. Phys. B* 871 (2013) 1–20, arXiv:1302.2864 [hep-ex].
- [13] R. Maciula, A. Szczurek, Production of Λ_c baryons at the LHC within the k_T -factorization approach and independent parton fragmentation picture, *Phys. Rev. D* 98 (1) (2018) 014016, arXiv:1803.05807 [hep-ph].
- [14] LHCb Collaboration, R. Aaij, et al., Prompt Λ_c^+ production in pPb collisions at $\sqrt{s_{NN}} = 5.02$ TeV, *J. High Energy Phys.* 02 (2019) 102, arXiv:1809.01404 [hep-ex].
- [15] H.-H. Li, F.-L. Shao, J. Song, R.-Q. Wang, Production of single-charm hadrons by quark combination mechanism in p–Pb collisions at $\sqrt{s_{NN}} = 5.02$ TeV, *Phys. Rev. C* 97 (6) (2018) 064915, arXiv:1712.08921 [hep-ph].
- [16] J. Song, H.-h. Li, F.-L. Shao, New feature of low p_T charm quark hadronization in pp collisions at $\sqrt{s} = 7$ TeV, *Eur. Phys. J. C* 78 (4) (2018) 344, arXiv:1801.09402 [hep-ph].
- [17] ALICE Collaboration, K. Aamodt, et al., The ALICE experiment at the CERN LHC, *J. Instrum.* 3 (2008) S08002.
- [18] ALICE Collaboration, S. Acharya, et al., Measurement of D^0 , D^+ , D^{*+} and D_s^+ production in Pb–Pb collisions at $\sqrt{s_{NN}} = 5.02$ TeV, Submitted to *J. High Energy Phys.* (2018), arXiv:1804.09083 [nucl-ex].
- [19] Particle Data Group Collaboration, M. Tanabashi, et al., Review of particle physics, *Phys. Rev. D* 98 (2018) 030001.
- [20] ALICE Collaboration, B. Abelev, et al., Performance of the ALICE experiment at the CERN LHC, *Int. J. Mod. Phys. A* 29 (2014) 1430044, arXiv:1402.4476 [nucl-ex].
- [21] ALICE Collaboration, K. Aamodt, et al., Alignment of the ALICE inner tracking system with cosmic-ray tracks, *J. Instrum.* 5 (2010) P03003, arXiv:1001.0502 [physics.ins-det].
- [22] J. Alme, et al., The ALICE TPC, a large 3-dimensional tracking device with fast readout for ultra-high multiplicity events, *Nucl. Instrum. Methods A* 622 (2010) 316–367, arXiv:1001.1950 [physics.ins-det].
- [23] A. Akimov, et al., Performance of the ALICE time-of-flight detector at the LHC, *Eur. Phys. J. Plus* 128 (2013) 44.
- [24] ALICE Collaboration, E. Abbas, et al., Performance of the ALICE VZERO system, *J. Instrum.* 8 (2013) P10016, arXiv:1306.3130 [nucl-ex].
- [25] ALICE Collaboration, Centrality determination in heavy ion collisions, 2018, ALICE-PUBLIC-2018-011.
- [26] J. Podolanski, R. Armenteros, III. Analysis of V-events, *Phys. Mag.* 45 (1954) 13–30.
- [27] ALICE Collaboration, B. Abelev, et al., Azimuthal anisotropy of D meson production in Pb–Pb collisions at $\sqrt{s_{NN}} = 2.76$ TeV, *Phys. Rev. C* 90 (3) (2014) 034904, arXiv:1405.2001 [nucl-ex].
- [28] X.-N. Wang, M. Gyulassy, HIJING: a Monte Carlo model for multiple jet production in pp, pA and AA collisions, *Phys. Rev. D* 44 (1991) 3501–3516.
- [29] T. Sjostrand, S. Mrenna, P.Z. Skands, PYTHIA 6.4 physics and manual, *J. High Energy Phys.* 05 (2006) 026, arXiv:hep-ph/0603175 [hep-ph].
- [30] R. Brun, F. Bruyant, F. Carminati, S. Giani, M. Maire, A. McPherson, G. Patrick, L. Urban, GEANT Detector Description and Simulation Tool, CERN Program Library Long Writeup CERN-W5013, 1994.
- [31] M. Cacciari, M. Greco, P. Nason, The p_T spectrum in heavy flavor hadroproduction, *J. High Energy Phys.* 05 (1998) 007, arXiv:hep-ph/9803400 [hep-ph].
- [32] M. Cacciari, S. Frixione, P. Nason, The p_T spectrum in heavy flavor photoproduction, *J. High Energy Phys.* 03 (2001) 006, arXiv:hep-ph/0102134 [hep-ph].
- [33] ALICE Collaboration, B. Abelev, et al., Measurement of charm production at central rapidity in proton–proton collisions at $\sqrt{s} = 7$ TeV, *J. High Energy Phys.* 01 (2012) 128, arXiv:1111.1553 [hep-ex].
- [34] L. Gladilin, Fragmentation fractions of c and b quarks into charmed hadrons at LEP, *Eur. Phys. J. C* 75 (1) (2015) 19, arXiv:1404.3888 [hep-ex].
- [35] D.J. Lange, The EvtGen particle decay simulation package, *Nucl. Instrum. Methods A* 462 (2001) 152–155.
- [36] M.L. Miller, K. Reygers, S.J. Sanders, P. Steinberg, Glauber modeling in high energy nuclear collisions, *Annu. Rev. Nucl. Part. Sci.* 57 (2007) 205–243, arXiv:nucl-ex/0701025.
- [37] C. Loizides, J. Kamin, D. d’Enterria, Improved Monte Carlo Glauber predictions at present and future nuclear colliders, *Phys. Rev. C* 97 (5) (2018) 054910, arXiv:1710.07098 [nucl-ex].
- [38] CMS Collaboration, V. Khachatryan, et al., Suppression and azimuthal anisotropy of prompt and nonprompt J/ψ production in PbPb collisions at $\sqrt{s_{NN}} = 2.76$ TeV, *Eur. Phys. J. C* 77 (4) (2017) 252, arXiv:1610.00613 [nucl-ex].
- [39] CMS Collaboration, A.M. Sirunyan, et al., Nuclear modification factor of D^0 mesons in PbPb collisions at $\sqrt{s_{NN}} = 5.02$ TeV, *Phys. Lett. B* 782 (2018) 474–496, arXiv:1708.04962 [nucl-ex].
- [40] S.K. Das, J.M. Torres-Rincon, L. Tolos, V. Minissale, F. Scardina, V. Greco, Propagation of heavy baryons in heavy-ion collisions, *Phys. Rev. D* 94 (11) (2016) 114039, arXiv:1604.05666 [nucl-th].
- [41] G. Martinez-Garcia, S. Gadrat, P. Crochet, Consequences of a Λ_c/D enhancement effect on the non-photonuclear electron nuclear modification factor in central heavy ion collisions at RHIC energy, *Phys. Lett. B* 663 (2008) 55–60, arXiv:0710.2152 [hep-ph], Erratum: *Phys. Lett. B* 666 (2008) 533.
- [42] ALICE Collaboration, S. Acharya, et al., Transverse momentum spectra and nuclear modification factors of charged particles in pp, p–Pb and Pb–Pb collisions at the LHC, *J. High Energy Phys.* 1811 (2018) 013, arXiv:1802.09145 [nucl-ex].
- [43] STAR Collaboration, G. Xie, Λ_c production in Au+Au collisions at $\sqrt{s_{NN}} = 200$ GeV measured by the STAR experiment, *Nucl. Phys. A* 967 (2017) 928–931, arXiv:1704.04353 [nucl-ex].
- [44] ALICE Collaboration, S. Acharya, et al., Measurement of D-meson production at mid-rapidity in pp collisions at $\sqrt{s} = 7$ TeV, *Eur. Phys. J. C* 77 (8) (2017) 550, arXiv:1702.00766 [hep-ex].
- [45] ALICE Collaboration, B. Abelev, et al., Upgrade of the ALICE experiment: letter of intent, *J. Phys. G* 41 (2014) 087001.
- [46] ALICE Collaboration, B. Abelev, et al., Technical design report for the upgrade of the ALICE inner tracking system, *J. Phys. G* 41 (2014) 087002.

ALICE Collaboration

S. Acharya¹⁴⁰, F.T. Acosta²⁰, D. Adamová⁹³, S.P. Adhya¹⁴⁰, A. Adler⁷⁴, J. Adolfsson⁸⁰, M.M. Aggarwal⁹⁸, G. Aglieri Rinella³⁴, M. Agnello³¹, N. Agrawal⁴⁸, Z. Ahammed¹⁴⁰, S. Ahmad¹⁷, S.U. Ahn⁷⁶, S. Aiola¹⁴⁵,

A. Akindinov⁶⁴, M. Al-Turany¹⁰⁴, S.N. Alam¹⁴⁰, D.S.D. Albuquerque¹²¹, D. Aleksandrov⁸⁷, B. Alessandro⁵⁸, H.M. Alfanda⁶, R. Alfaro Molina⁷², Y. Ali¹⁵, A. Alici^{10,53,27}, A. Alkin², J. Alme²², T. Alt⁶⁹, L. Altenkamper²², I. Altsybeev¹¹¹, M.N. Anaam⁶, C. Andrei⁴⁷, D. Andreou³⁴, H.A. Andrews¹⁰⁸, A. Andronic^{104,143}, M. Angeletti³⁴, V. Anguelov¹⁰², C. Anson¹⁶, T. Antičić¹⁰⁵, F. Antinori⁵⁶, P. Antonioli⁵³, R. Anwar¹²⁵, N. Apadula⁷⁹, L. Aphecetche¹¹³, H. Appelshäuser⁶⁹, S. Arcelli²⁷, R. Arnaldi⁵⁸, M. Arratia⁷⁹, I.C. Arsene²¹, M. Arslanok¹⁰², A. Augustinus³⁴, R. Averbeck¹⁰⁴, M.D. Azmi¹⁷, A. Badalà⁵⁵, Y.W. Baek^{60,40}, S. Bagnasco⁵⁸, R. Bailhache⁶⁹, R. Bala⁹⁹, A. Baldisseri¹³⁶, M. Ball⁴², R.C. Baral⁸⁵, R. Barbera²⁸, L. Barioglio²⁶, G.G. Barnaföldi¹⁴⁴, L.S. Barnby⁹², V. Barret¹³³, P. Bartalini⁶, K. Barth³⁴, E. Bartsch⁶⁹, N. Bastid¹³³, S. Basu¹⁴², G. Batigne¹¹³, B. Batyunya⁷⁵, P.C. Batzing²¹, J.L. Bazo Alba¹⁰⁹, I.G. Bearden⁸⁸, H. Beck¹⁰², C. Bedda⁶³, N.K. Behera⁶⁰, I. Belikov¹³⁵, F. Bellini³⁴, H. Bello Martinez⁴⁴, R. Bellwied¹²⁵, L.G.E. Beltran¹¹⁹, V. Belyaev⁹¹, G. Bencedi¹⁴⁴, S. Beole²⁶, A. Bercuci⁴⁷, Y. Berdnikov⁹⁶, D. Berenyi¹⁴⁴, R.A. Bertens¹²⁹, D. Berzano^{58,34}, L. Betev³⁴, A. Bhasin⁹⁹, I.R. Bhat⁹⁹, H. Bhatt⁴⁸, B. Bhattacharjee⁴¹, J. Bhom¹¹⁷, A. Bianchi²⁶, L. Bianchi^{125,26}, N. Bianchi⁵¹, J. Bielčik³⁷, J. Bielčíková⁹³, A. Bilandzic^{103,116}, G. Biro¹⁴⁴, R. Biswas³, S. Biswas³, J.T. Blair¹¹⁸, D. Blau⁸⁷, C. Blume⁶⁹, G. Boca¹³⁸, F. Bock³⁴, A. Bogdanov⁹¹, L. Boldizsár¹⁴⁴, A. Bolozdynya⁹¹, M. Bombara³⁸, G. Bonomi¹³⁹, M. Bonora³⁴, H. Borel¹³⁶, A. Borissov^{143,102}, M. Borri¹²⁷, E. Botta²⁶, C. Bourjau⁸⁸, L. Bratrud⁶⁹, P. Braun-Munzinger¹⁰⁴, M. Bregant¹²⁰, T.A. Broker⁶⁹, M. Broz³⁷, E.J. Brucken⁴³, E. Bruna⁵⁸, G.E. Bruno³³, D. Budnikov¹⁰⁶, H. Buesching⁶⁹, S. Bufalino³¹, P. Buhler¹¹², P. Buncic³⁴, O. Busch^{132,i}, Z. Buthelezi⁷³, J.B. Butt¹⁵, J.T. Buxton⁹⁵, J. Cabala¹¹⁵, D. Caffarri⁸⁹, H. Caines¹⁴⁵, A. Caliva¹⁰⁴, E. Calvo Villar¹⁰⁹, R.S. Camacho⁴⁴, P. Camerini²⁵, A.A. Capon¹¹², F. Carnesecchi^{27,10}, J. Castillo Castellanos¹³⁶, A.J. Castro¹²⁹, E.A.R. Casula⁵⁴, C. Ceballos Sanchez⁸, S. Chandra¹⁴⁰, B. Chang¹²⁶, W. Chang⁶, S. Chapeland³⁴, M. Chartier¹²⁷, S. Chattopadhyay¹⁴⁰, S. Chattopadhyay¹⁰⁷, A. Chauvin²⁴, C. Cheshkov¹³⁴, B. Cheynis¹³⁴, V. Chibante Barroso³⁴, D.D. Chinellato¹²¹, S. Cho⁶⁰, P. Chochula³⁴, T. Chowdhury¹³³, P. Christakoglou⁸⁹, C.H. Christensen⁸⁸, P. Christiansen⁸⁰, T. Chujo¹³², C. Cicalo⁵⁴, L. Cifarelli^{10,27}, F. Cindolo⁵³, J. Cleymans¹²⁴, F. Colamaria⁵², D. Colella⁵², A. Collu⁷⁹, M. Colocci²⁷, M. Concas^{58,ii}, G. Conesa Balbastre⁷⁸, Z. Conesa del Valle⁶¹, J.G. Contreras³⁷, T.M. Cormier⁹⁴, Y. Corrales Morales⁵⁸, P. Cortese³², M.R. Cosentino¹²², F. Costa³⁴, S. Costanza¹³⁸, J. Crkovská⁶¹, P. Crochet¹³³, E. Cuautle⁷⁰, L. Cunqueiro⁹⁴, D. Dabrowski¹⁴¹, T. Dahms^{103,116}, A. Dainese⁵⁶, F.P.A. Damas^{136,113}, S. Dani⁶⁶, M.C. Danisch¹⁰², A. Danu⁶⁸, D. Das¹⁰⁷, I. Das¹⁰⁷, S. Das³, A. Dash⁸⁵, S. Dash⁴⁸, S. De⁴⁹, A. De Caro³⁰, G. de Cataldo⁵², C. de Conti¹²⁰, J. de Cuveland³⁹, A. De Falco²⁴, D. De Gruttola^{10,30}, N. De Marco⁵⁸, S. De Pasquale³⁰, R.D. De Souza¹²¹, H.F. Degenhardt¹²⁰, A. Deisting^{102,104}, A. Deloff⁸⁴, S. Delsanto²⁶, P. Dhankher⁴⁸, D. Di Bari³³, A. Di Mauro³⁴, R.A. Diaz⁸, T. Dietel¹²⁴, P. Dillenseger⁶⁹, Y. Ding⁶, R. Divià³⁴, Ø. Djuvsland²², A. Dobrin³⁴, D. Domenicis Gimenez¹²⁰, B. Dönigus⁶⁹, O. Dordic²¹, A.K. Dubey¹⁴⁰, A. Dubla¹⁰⁴, S. Dudi⁹⁸, A.K. Duggal⁹⁸, M. Dukhishyam⁸⁵, P. Dupieux¹³³, R.J. Ehlers¹⁴⁵, D. Elia⁵², H. Engel⁷⁴, E. Eppe¹⁴⁵, B. Erasmus¹¹³, F. Erhardt⁹⁷, A. Erokhin¹¹¹, M.R. Ersdal²², B. Espagnon⁶¹, G. Eulisse³⁴, J. Eum¹⁸, D. Evans¹⁰⁸, S. Evdokimov⁹⁰, L. Fabbietti^{103,116}, M. Faggin²⁹, J. Faivre⁷⁸, A. Fantoni⁵¹, M. Fasel⁹⁴, L. Feldkamp¹⁴³, A. Feliciello⁵⁸, G. Feofilov¹¹¹, A. Fernández Téllez⁴⁴, A. Ferrero¹³⁶, A. Ferretti²⁶, A. Festanti³⁴, V.J.G. Feuillard¹⁰², J. Figiel¹¹⁷, S. Filchagin¹⁰⁶, D. Finogeev⁶², F.M. Fionda²², G. Fiorenza⁵², F. Flor¹²⁵, M. Floris³⁴, S. Foertsch⁷³, P. Foka¹⁰⁴, S. Fokin⁸⁷, E. Fragiaco⁵⁹, A. Francisco¹¹³, U. Frankenfeld¹⁰⁴, G.G. Fronze²⁶, U. Fuchs³⁴, C. Furget⁷⁸, A. Furs⁶², M. Fusco Girard³⁰, J.J. Gaardhøje⁸⁸, M. Gagliardi²⁶, A.M. Gago¹⁰⁹, K. Gajdosova^{37,88}, C.D. Galvan¹¹⁹, P. Ganoti⁸³, C. Garabatos¹⁰⁴, E. Garcia-Solis¹¹, K. Garg²⁸, C. Gargiulo³⁴, K. Garner¹⁴³, P. Gasik^{103,116}, E.F. Gauger¹¹⁸, M.B. Gay Ducati⁷¹, M. Germain¹¹³, J. Ghosh¹⁰⁷, P. Ghosh¹⁴⁰, S.K. Ghosh³, P. Gianotti⁵¹, P. Giubellino^{104,58}, P. Giubilato²⁹, P. Glässel¹⁰², D.M. Gómez Coral⁷², A. Gomez Ramirez⁷⁴, V. Gonzalez¹⁰⁴, P. González-Zamora⁴⁴, S. Gorbunov³⁹, L. Görlich¹¹⁷, S. Gotovac³⁵, V. Grabski⁷², L.K. Graczykowski¹⁴¹, K.L. Graham¹⁰⁸, L. Greiner⁷⁹, A. Grelli⁶³, C. Grigoras³⁴, V. Grigoriev⁹¹, A. Grigoryan¹, S. Grigoryan⁷⁵, J.M. Gronefeld¹⁰⁴, F. Groa³¹, J.F. Grosse-Oetringhaus³⁴, R. Grosso¹⁰⁴, R. Guernane⁷⁸, B. Guerzoni²⁷, M. Guittiere¹¹³, K. Gulbrandsen⁸⁸, T. Gunji¹³¹, A. Gupta⁹⁹, R. Gupta⁹⁹, I.B. Guzman⁴⁴, R. Haake^{145,34}, M.K. Habib¹⁰⁴, C. Hadjidakis⁶¹, H. Hamagaki⁸¹, G. Hamar¹⁴⁴, M. Hamid⁶, J.C. Hamon¹³⁵, R. Hannigan¹¹⁸, M.R. Haque⁶³, A. Harlenderova¹⁰⁴, J.W. Harris¹⁴⁵, A. Harton¹¹, H. Hassan⁷⁸, D. Hatzifotiadiou^{53,10},

P. Hauer⁴², S. Hayashi¹³¹, S.T. Heckel⁶⁹, E. Hellbär⁶⁹, H. Helstrup³⁶, A. Herghelegiu⁴⁷, E.G. Hernandez⁴⁴, G. Herrera Corral⁹, F. Herrmann¹⁴³, K.F. Hetland³⁶, T.E. Hilden⁴³, H. Hillemanns³⁴, C. Hills¹²⁷, B. Hippolyte¹³⁵, B. Hohlweger¹⁰³, D. Horak³⁷, S. Hornung¹⁰⁴, R. Hosokawa^{132,78}, J. Hota⁶⁶, P. Hristov³⁴, C. Huang⁶¹, C. Hughes¹²⁹, P. Huhn⁶⁹, T.J. Humanic⁹⁵, H. Hushnud¹⁰⁷, L.A. Husova¹⁴³, N. Hussain⁴¹, T. Hussain¹⁷, D. Hutter³⁹, D.S. Hwang¹⁹, J.P. Iddon¹²⁷, R. Ilkaev¹⁰⁶, M. Inaba¹³², M. Ippolitov⁸⁷, M.S. Islam¹⁰⁷, M. Ivanov¹⁰⁴, V. Ivanov⁹⁶, V. Izucheev⁹⁰, B. Jacak⁷⁹, N. Jacazio²⁷, P.M. Jacobs⁷⁹, M.B. Jadhav⁴⁸, S. Jadlovska¹¹⁵, J. Jadlovsky¹¹⁵, S. Jaelani⁶³, C. Jahnke^{120,116}, M.J. Jakubowska¹⁴¹, M.A. Janik¹⁴¹, M. Jercic⁹⁷, O. Jevons¹⁰⁸, R.T. Jimenez Bustamante¹⁰⁴, M. Jin¹²⁵, P.G. Jones¹⁰⁸, A. Jusko¹⁰⁸, P. Kalinak⁶⁵, A. Kalweit³⁴, J.H. Kang¹⁴⁶, V. Kaplin⁹¹, S. Kar⁶, A. Karasu Uysal⁷⁷, O. Karavichev⁶², T. Karavicheva⁶², P. Karczmarczyk³⁴, E. Karpechev⁶², U. Kebschull⁷⁴, R. Keidel⁴⁶, D.L.D. Keijdener⁶³, M. Keil³⁴, B. Ketzer⁴², Z. Khabanova⁸⁹, A.M. Khan⁶, S. Khan¹⁷, S.A. Khan¹⁴⁰, A. Khanzadeev⁹⁶, Y. Kharlov⁹⁰, A. Khatun¹⁷, A. Khuntia⁴⁹, M.M. Kielbowicz¹¹⁷, B. Kileng³⁶, B. Kim⁶⁰, B. Kim¹³², D. Kim¹⁴⁶, D.J. Kim¹²⁶, E.J. Kim¹³, H. Kim¹⁴⁶, J.S. Kim⁴⁰, J. Kim¹⁰², J. Kim¹³, M. Kim^{60,102}, S. Kim¹⁹, T. Kim¹⁴⁶, T. Kim¹⁴⁶, K. Kindra⁹⁸, S. Kirsch³⁹, I. Kisel³⁹, S. Kiselev⁶⁴, A. Kisiel¹⁴¹, J.L. Klay⁵, C. Klein⁶⁹, J. Klein⁵⁸, C. Klein-Bösing¹⁴³, S. Klewin¹⁰², A. Kluge³⁴, M.L. Knichel³⁴, A.G. Knospe¹²⁵, C. Kobdaj¹¹⁴, M. Kofarago¹⁴⁴, M.K. Köhler¹⁰², T. Kollegger¹⁰⁴, N. Kondratyeva⁹¹, E. Kondratyuk⁹⁰, A. Konevskikh⁶², P.J. Konopka³⁴, M. Konyushikhin¹⁴², L. Koska¹¹⁵, O. Kovalenko⁸⁴, V. Kovalenko¹¹¹, M. Kowalski¹¹⁷, I. Králik⁶⁵, A. Kravčáková³⁸, L. Kreis¹⁰⁴, M. Krivda^{108,65}, F. Krizek⁹³, M. Krüger⁶⁹, E. Kryshen⁹⁶, M. Krzewicki³⁹, A.M. Kubera⁹⁵, V. Kučera^{93,60}, C. Kuhn¹³⁵, P.G. Kuijer⁸⁹, J. Kumar⁴⁸, L. Kumar⁹⁸, S. Kumar⁴⁸, S. Kundu⁸⁵, P. Kurashvili⁸⁴, A. Kurepin⁶², A.B. Kurepin⁶², S. Kushpil⁹³, J. Kvapil¹⁰⁸, M.J. Kweon⁶⁰, Y. Kwon¹⁴⁶, S.L. La Pointe³⁹, P. La Rocca²⁸, Y.S. Lai⁷⁹, I. Lakomov³⁴, R. Langoy¹²³, K. Lapidus^{145,34}, A. Lardeux²¹, P. Larionov⁵¹, E. Laudi³⁴, R. Lavicka³⁷, T. Lazareva¹¹¹, R. Lea²⁵, L. Leardini¹⁰², S. Lee¹⁴⁶, F. Lehas⁸⁹, S. Lehner¹¹², J. Lehrbach³⁹, R.C. Lemmon⁹², I. León Monzón¹¹⁹, P. Lévai¹⁴⁴, X. Li¹², X.L. Li⁶, J. Lien¹²³, R. Lietava¹⁰⁸, B. Lim¹⁸, S. Lindal²¹, V. Lindenstruth³⁹, S.W. Lindsay¹²⁷, C. Lippmann¹⁰⁴, M.A. Lisa⁹⁵, V. Litichevskiy⁴³, A. Liu⁷⁹, H.M. Ljunggren⁸⁰, W.J. Llope¹⁴², D.F. Lodato⁶³, V. Loginov⁹¹, C. Loizides⁹⁴, P. Loncar³⁵, X. Lopez¹³³, E. López Torres⁸, P. Luettig⁶⁹, J.R. Luhder¹⁴³, M. Lunardon²⁹, G. Luparello⁵⁹, M. Lupi³⁴, A. Maevskaya⁶², M. Mager³⁴, S.M. Mahmood²¹, A. Maire¹³⁵, R.D. Majka¹⁴⁵, M. Malaev⁹⁶, Q.W. Malik²¹, L. Malinina^{75,iii}, D. Mal'Kevich⁶⁴, P. Malzacher¹⁰⁴, A. Mamonov¹⁰⁶, V. Manko⁸⁷, F. Manso¹³³, V. Manzari⁵², Y. Mao⁶, M. Marchisone¹³⁴, J. Mareš⁶⁷, G.V. Margagliotti²⁵, A. Margotti⁵³, J. Margutti⁶³, A. Marín¹⁰⁴, C. Markert¹¹⁸, M. Marquard⁶⁹, N.A. Martin^{102,104}, P. Martinengo³⁴, J.L. Martinez¹²⁵, M.I. Martínez⁴⁴, G. Martínez García¹¹³, M. Martinez Pedreira³⁴, S. Masciocchi¹⁰⁴, M. Masera²⁶, A. Masoni⁵⁴, L. Massacrier⁶¹, E. Masson¹¹³, A. Mastroserio^{52,137}, A.M. Mathis^{116,103}, P.F.T. Matuoka¹²⁰, A. Matyja^{117,129}, C. Mayer¹¹⁷, M. Mazzilli³³, M.A. Mazzoni⁵⁷, F. Meddi²³, Y. Melikyan⁹¹, A. Menchaca-Rocha⁷², E. Meninno³⁰, M. Meres¹⁴, S. Mhlanga¹²⁴, Y. Miake¹³², L. Micheletti²⁶, M.M. Mieskolainen⁴³, D.L. Mihaylov¹⁰³, K. Mikhaylov^{75,64}, A. Mischke⁶³, A.N. Mishra⁷⁰, D. Miśkowiec¹⁰⁴, J. Mitra¹⁴⁰, C.M. Mitu⁶⁸, N. Mohammadi³⁴, A.P. Mohanty⁶³, B. Mohanty⁸⁵, M. Mohisin Khan^{17,iv}, M.M. Mondal⁶⁶, C. Mordasini¹⁰³, D.A. Moreira De Godoy¹⁴³, L.A.P. Moreno⁴⁴, S. Moretto²⁹, A. Morreale¹¹³, A. Morsch³⁴, T. Mrnjavac³⁴, V. Muccifora⁵¹, E. Mudnic³⁵, D. Mühlheim¹⁴³, S. Muhuri¹⁴⁰, J.D. Mulligan¹⁴⁵, M.G. Munhoz¹²⁰, K. Munning⁴², R.H. Munzer⁶⁹, H. Murakami¹³¹, S. Murray⁷³, L. Musa³⁴, J. Musinsky⁶⁵, C.J. Myers¹²⁵, J.W. Myrcha¹⁴¹, B. Naik⁴⁸, R. Nair⁸⁴, B.K. Nandi⁴⁸, R. Nania^{53,10}, E. Nappi⁵², M.U. Naru¹⁵, A.F. Nassirpour⁸⁰, H. Natal da Luz¹²⁰, C. Nattrass¹²⁹, S.R. Navarro⁴⁴, K. Nayak⁸⁵, R. Nayak⁴⁸, T.K. Nayak^{140,85}, S. Nazarenko¹⁰⁶, R.A. Negrao De Oliveira⁶⁹, L. Nellen⁷⁰, S.V. Nesbo³⁶, G. Neskovic³⁹, F. Ng¹²⁵, J. Niedziela^{141,34}, B.S. Nielsen⁸⁸, S. Nikolaev⁸⁷, S. Nikulin⁸⁷, V. Nikulin⁹⁶, F. Noferini^{10,53}, P. Nomokonov⁷⁵, G. Nooren⁶³, J.C.C. Noris⁴⁴, J. Norman⁷⁸, A. Nyanin⁸⁷, J. Nystrand²², M. Ogino⁸¹, A. Ohlson¹⁰², J. Oleniacz¹⁴¹, A.C. Oliveira Da Silva¹²⁰, M.H. Oliver¹⁴⁵, J. Onderwaater¹⁰⁴, C. Oppedisano⁵⁸, R. Orava⁴³, M. Oravec¹¹⁵, A. Ortiz Velasquez⁷⁰, A. Oskarsson⁸⁰, J. Otwinowski¹¹⁷, K. Oyama⁸¹, Y. Pachmayer¹⁰², V. Pacik⁸⁸, D. Pagano¹³⁹, G. Paic⁷⁰, P. Palni⁶, J. Pan¹⁴², A.K. Pandey⁴⁸, S. Panebianco¹³⁶, V. Papikyan¹, P. Pareek⁴⁹, J. Park⁶⁰, J.E. Parkkila¹²⁶, S. Parmar⁹⁸, A. Passfeld¹⁴³, S.P. Pathak¹²⁵, R.N. Patra¹⁴⁰, B. Paul⁵⁸, H. Pei⁶, T. Peitzmann⁶³, X. Peng⁶, L.G. Pereira⁷¹, H. Pereira Da Costa¹³⁶, D. Peresunko⁸⁷, E. Perez Lezama⁶⁹, V. Peskov⁶⁹, Y. Pestov⁴, V. Petráček³⁷, M. Petrovici⁴⁷, R.P. Pezzi⁷¹, S. Piano⁵⁹, M. Pikna¹⁴, P. Pillot¹¹³,

L.O.D.L. Pimentel⁸⁸, O. Pinazza^{53,34}, L. Pinsky¹²⁵, S. Pisano⁵¹, D.B. Piyarathna¹²⁵, M. Płoskoń⁷⁹, M. Planinic⁹⁷, F. Pliquett⁶⁹, J. Pluta¹⁴¹, S. Pochybova¹⁴⁴, P.L.M. Podesta-Lerma¹¹⁹, M.G. Poghosyan⁹⁴, B. Polichtchouk⁹⁰, N. Poljak⁹⁷, W. Poonsawat¹¹⁴, A. Pop⁴⁷, H. Poppenborg¹⁴³, S. Porteboeuf-Houssais¹³³, V. Pozdniakov⁷⁵, S.K. Prasad³, R. Preghenella⁵³, F. Prino⁵⁸, C.A. Pruneau¹⁴², I. Pshenichnov⁶², M. Puccio²⁶, V. Punin¹⁰⁶, K. Puranapanda¹⁴⁰, J. Putschke¹⁴², R.E. Quishpe¹²⁵, S. Raha³, S. Rajput⁹⁹, J. Rak¹²⁶, A. Rakotozafindrabe¹³⁶, L. Ramello³², F. Rami¹³⁵, R. Raniwala¹⁰⁰, S. Raniwala¹⁰⁰, S.S. Räsänen⁴³, B.T. Rascanu⁶⁹, R. Rath⁴⁹, V. Ratza⁴², I. Ravasenga³¹, K.F. Read^{94,129}, K. Redlich^{84,v}, A. Rehman²², P. Reichelt⁶⁹, F. Reidt³⁴, X. Ren⁶, R. Renfordt⁶⁹, A. Reshetin⁶², J.-P. Revol¹⁰, K. Reygers¹⁰², V. Riabov⁹⁶, T. Richert^{88,80}, M. Richter²¹, P. Riedler³⁴, W. Riegler³⁴, F. Riggi²⁸, C. Ristea⁶⁸, S.P. Rode⁴⁹, M. Rodríguez Cahuantzi⁴⁴, K. Røed²¹, R. Rogalev⁹⁰, E. Rogochaya⁷⁵, D. Rohr³⁴, D. Röhrich²², P.S. Rokita¹⁴¹, F. Ronchetti⁵¹, E.D. Rosas⁷⁰, K. Roslon¹⁴¹, P. Rosnet¹³³, A. Rossi^{56,29}, A. Rotondi¹³⁸, F. Roukoutakis⁸³, A. Roy⁴⁹, P. Roy¹⁰⁷, O.V. Rueda⁷⁰, R. Rui²⁵, B. Rumyantsev⁷⁵, A. Rustamov⁸⁶, E. Ryabinkin⁸⁷, Y. Ryabov⁹⁶, A. Rybicki¹¹⁷, S. Saarinen⁴³, S. Sadhu¹⁴⁰, S. Sadovsky⁹⁰, K. Šafařík³⁴, S.K. Saha¹⁴⁰, B. Sahoo⁴⁸, P. Sahoo⁴⁹, R. Sahoo⁴⁹, S. Sahoo⁶⁶, P.K. Sahu⁶⁶, J. Saini¹⁴⁰, S. Sakai¹³², M.A. Saleh¹⁴², S. Sambyal⁹⁹, V. Samsonov^{91,96}, A. Sandoval⁷², A. Sarkar⁷³, D. Sarkar¹⁴⁰, N. Sarkar¹⁴⁰, P. Sarma⁴¹, V.M. Sarti¹⁰³, M.H.P. Sas⁶³, E. Scapparone⁵³, B. Schaefer⁹⁴, J. Schambach¹¹⁸, H.S. Scheid⁶⁹, C. Schiaua⁴⁷, R. Schicker¹⁰², C. Schmidt¹⁰⁴, H.R. Schmidt¹⁰¹, M.O. Schmidt¹⁰², M. Schmidt¹⁰¹, N.V. Schmidt^{94,69}, J. Schukraft^{34,88}, Y. Schutz^{34,135}, K. Schwarz¹⁰⁴, K. Schweda¹⁰⁴, G. Scioli²⁷, E. Scomparin⁵⁸, M. Šefčík³⁸, J.E. Seger¹⁶, Y. Sekiguchi¹³¹, D. Sekihata⁴⁵, I. Selyuzhenkov^{91,104}, S. Senyukov¹³⁵, E. Serradilla⁷², P. Sett⁴⁸, A. Sevcenco⁶⁸, A. Shabanov⁶², A. Shabetai¹¹³, R. Shahoyan³⁴, W. Shaikh¹⁰⁷, A. Shangaraev⁹⁰, A. Sharma⁹⁸, A. Sharma⁹⁹, M. Sharma⁹⁹, N. Sharma⁹⁸, A.I. Sheikh¹⁴⁰, K. Shigaki⁴⁵, M. Shimomura⁸², S. Shirinkin⁶⁴, Q. Shou^{6,110}, Y. Sibiriak⁸⁷, S. Siddhanta⁵⁴, T. Siemiarczuk⁸⁴, D. Silvermyr⁸⁰, G. Simatovic⁸⁹, G. Simonetti^{103,34}, R. Singh⁸⁵, R. Singh⁹⁹, V. Singhal¹⁴⁰, T. Sinha¹⁰⁷, B. Sitar¹⁴, M. Sitta³², T.B. Skaali²¹, M. Slupecki¹²⁶, N. Smirnov¹⁴⁵, R.J.M. Snellings⁶³, T.W. Snellman¹²⁶, J. Sochan¹¹⁵, C. Soncco¹⁰⁹, J. Song⁶⁰, A. Songmoolnak¹¹⁴, F. Soramel²⁹, S. Sorensen¹²⁹, F. Sozzi¹⁰⁴, I. Sputowska¹¹⁷, J. Stachel¹⁰², I. Stan⁶⁸, P. Stankus⁹⁴, E. Stenlund⁸⁰, D. Stocco¹¹³, M.M. Storetvedt³⁶, P. Strmen¹⁴, A.A.P. Suaide¹²⁰, T. Sugitate⁴⁵, C. Suire⁶¹, M. Suleymanov¹⁵, M. Suljic³⁴, R. Sultanov⁶⁴, M. Šumbera⁹³, S. Sumowidagdo⁵⁰, K. Suzuki¹¹², S. Swain⁶⁶, A. Szabo¹⁴, I. Szarka¹⁴, U. Tabassam¹⁵, J. Takahashi¹²¹, G.J. Tambave²², N. Tanaka¹³², M. Tarhini¹¹³, M.G. Tarzila⁴⁷, A. Tauro³⁴, G. Tejeda Muñoz⁴⁴, A. Telesca³⁴, C. Terrevoli^{29,125}, D. Thakur⁴⁹, S. Thakur¹⁴⁰, D. Thomas¹¹⁸, F. Thoresen⁸⁸, R. Tieulent¹³⁴, A. Tikhonov⁶², A.R. Timmins¹²⁵, A. Toia⁶⁹, N. Topilskaya⁶², M. Toppi⁵¹, S.R. Torres¹¹⁹, S. Tripathy⁴⁹, S. Trogolo²⁶, G. Trombetta³³, L. Tropp³⁸, V. Trubnikov², W.H. Trzaska¹²⁶, T.P. Trzcinski¹⁴¹, B.A. Trzeciak⁶³, T. Tsuji¹³¹, A. Tumkin¹⁰⁶, R. Turrisi⁵⁶, T.S. Tveter²¹, K. Ullaland²², E.N. Umaka¹²⁵, A. Uras¹³⁴, G.L. Usai²⁴, A. Utrobicic⁹⁷, M. Vala^{38,115}, L. Valencia Palomo⁴⁴, N. Valle¹³⁸, N. van der Kolk⁶³, L.V.R. van Doremalen⁶³, J.W. Van Hoorne³⁴, M. van Leeuwen⁶³, P. Vande Vyvre³⁴, D. Varga¹⁴⁴, A. Vargas⁴⁴, M. Vargyas¹²⁶, R. Varma⁴⁸, M. Vasileiou⁸³, A. Vasiliev⁸⁷, O. Vázquez Doce^{103,116}, V. Vechernin¹¹¹, A.M. Veen⁶³, E. Vercellin²⁶, S. Vergara Limón⁴⁴, L. Vermunt⁶³, R. Vernet⁷, R. Vértesi¹⁴⁴, L. Vickovic³⁵, J. Viinikainen¹²⁶, Z. Vilakazi¹³⁰, O. Villalobos Baillie¹⁰⁸, A. Villatoro Tello⁴⁴, G. Vino⁵², A. Vinogradov⁸⁷, T. Virgili³⁰, V. Vislavicius^{80,88}, A. Vodopyanov⁷⁵, B. Volke³⁴, M.A. Völkl¹⁰¹, K. Voloshin⁶⁴, S.A. Voloshin¹⁴², G. Volpe³³, B. von Haller³⁴, I. Vorobyev^{116,103}, D. Voscek¹¹⁵, J. Vrláková³⁸, B. Wagner²², M. Wang⁶, Y. Watanabe¹³², M. Weber¹¹², S.G. Weber¹⁰⁴, A. Wegrzynek³⁴, D.F. Weiser¹⁰², S.C. Wenzel³⁴, J.P. Wessels¹⁴³, U. Westerhoff¹⁴³, A.M. Whitehead¹²⁴, E. Widmann¹¹², J. Wiechula⁶⁹, J. Wikne²¹, G. Wilk⁸⁴, J. Wilkinson⁵³, G.A. Willems^{143,34}, E. Willsher¹⁰⁸, B. Windelband¹⁰², W.E. Witt¹²⁹, Y. Wu¹²⁸, R. Xu⁶, S. Yalcin⁷⁷, K. Yamakawa⁴⁵, S. Yano^{136,45}, Z. Yin⁶, H. Yokoyama^{63,132,78}, I.-K. Yoo¹⁸, J.H. Yoon⁶⁰, S. Yuan²², V. Yurchenko², V. Zaccolo^{58,25}, A. Zaman¹⁵, C. Zampolli³⁴, H.J.C. Zanoli¹²⁰, N. Zardoshti¹⁰⁸, A. Zarochentsev¹¹¹, P. Závada⁶⁷, N. Zaviyalov¹⁰⁶, H. Zbroszczyk¹⁴¹, M. Zhalov⁹⁶, X. Zhang⁶, Y. Zhang⁶, Z. Zhang^{6,133}, C. Zhao²¹, V. Zhrebchevskii¹¹¹, N. Zhigareva⁶⁴, D. Zhou⁶, Y. Zhou⁸⁸, Z. Zhou²², H. Zhu⁶, J. Zhu⁶, Y. Zhu⁶, A. Zichichi^{27,10}, M.B. Zimmermann³⁴, G. Zinovjev², N. Zurlo¹³⁹

¹ A.I. Alikhanyan National Science Laboratory (Yerevan Physics Institute) Foundation, Yerevan, Armenia

² Bogolyubov Institute for Theoretical Physics, National Academy of Sciences of Ukraine, Kiev, Ukraine

³ Bose Institute, Department of Physics and Centre for Astroparticle Physics and Space Science (CAPSS), Kolkata, India

- ⁴ Budker Institute for Nuclear Physics, Novosibirsk, Russia
- ⁵ California Polytechnic State University, San Luis Obispo, CA, United States
- ⁶ Central China Normal University, Wuhan, China
- ⁷ Centre de Calcul de l'IN2P3, Villeurbanne, Lyon, France
- ⁸ Centro de Aplicaciones Tecnológicas y Desarrollo Nuclear (CEADEN), Havana, Cuba
- ⁹ Centro de Investigación y de Estudios Avanzados (CINVESTAV), Mexico City and Mérida, Mexico
- ¹⁰ Centro Fermi - Museo Storico della Fisica e Centro Studi e Ricerche 'Enrico Fermi', Rome, Italy
- ¹¹ Chicago State University, Chicago, IL, United States
- ¹² China Institute of Atomic Energy, Beijing, China
- ¹³ Chonbuk National University, Jeonju, Republic of Korea
- ¹⁴ Comenius University Bratislava, Faculty of Mathematics, Physics and Informatics, Bratislava, Slovakia
- ¹⁵ COMSATS Institute of Information Technology (CIIT), Islamabad, Pakistan
- ¹⁶ Creighton University, Omaha, NE, United States
- ¹⁷ Department of Physics, Aligarh Muslim University, Aligarh, India
- ¹⁸ Department of Physics, Pusan National University, Pusan, Republic of Korea
- ¹⁹ Department of Physics, Sejong University, Seoul, Republic of Korea
- ²⁰ Department of Physics, University of California, Berkeley, CA, United States
- ²¹ Department of Physics, University of Oslo, Oslo, Norway
- ²² Department of Physics and Technology, University of Bergen, Bergen, Norway
- ²³ Dipartimento di Fisica dell'Università 'La Sapienza' and Sezione INFN, Rome, Italy
- ²⁴ Dipartimento di Fisica dell'Università and Sezione INFN, Cagliari, Italy
- ²⁵ Dipartimento di Fisica dell'Università and Sezione INFN, Trieste, Italy
- ²⁶ Dipartimento di Fisica dell'Università and Sezione INFN, Turin, Italy
- ²⁷ Dipartimento di Fisica e Astronomia dell'Università and Sezione INFN, Bologna, Italy
- ²⁸ Dipartimento di Fisica e Astronomia dell'Università and Sezione INFN, Catania, Italy
- ²⁹ Dipartimento di Fisica e Astronomia dell'Università and Sezione INFN, Padova, Italy
- ³⁰ Dipartimento di Fisica 'E.R. Caianiello' dell'Università and Gruppo Collegato INFN, Salerno, Italy
- ³¹ Dipartimento DISAT del Politecnico and Sezione INFN, Turin, Italy
- ³² Dipartimento di Scienze e Innovazione Tecnologica dell'Università del Piemonte Orientale and INFN Sezione di Torino, Alessandria, Italy
- ³³ Dipartimento Interateneo di Fisica 'M. Merlin' and Sezione INFN, Bari, Italy
- ³⁴ European Organization for Nuclear Research (CERN), Geneva, Switzerland
- ³⁵ Faculty of Electrical Engineering, Mechanical Engineering and Naval Architecture, University of Split, Split, Croatia
- ³⁶ Faculty of Engineering and Science, Western Norway University of Applied Sciences, Bergen, Norway
- ³⁷ Faculty of Nuclear Sciences and Physical Engineering, Czech Technical University in Prague, Prague, Czech Republic
- ³⁸ Faculty of Science, P.J. Šafárik University, Košice, Slovakia
- ³⁹ Frankfurt Institute for Advanced Studies, Johann Wolfgang Goethe-Universität Frankfurt, Frankfurt, Germany
- ⁴⁰ Gangneung-Wonju National University, Gangneung, Republic of Korea
- ⁴¹ Gauhati University, Department of Physics, Guwahati, India
- ⁴² Helmholtz-Institut für Strahlen- und Kernphysik, Rheinische Friedrich-Wilhelms-Universität Bonn, Bonn, Germany
- ⁴³ Helsinki Institute of Physics (HIP), Helsinki, Finland
- ⁴⁴ High Energy Physics Group, Universidad Autónoma de Puebla, Puebla, Mexico
- ⁴⁵ Hiroshima University, Hiroshima, Japan
- ⁴⁶ Hochschule Worms, Zentrum für Technologietransfer und Telekommunikation (ZTT), Worms, Germany
- ⁴⁷ Horia Hulubei National Institute of Physics and Nuclear Engineering, Bucharest, Romania
- ⁴⁸ Indian Institute of Technology Bombay (IIT), Mumbai, India
- ⁴⁹ Indian Institute of Technology Indore, Indore, India
- ⁵⁰ Indonesian Institute of Sciences, Jakarta, Indonesia
- ⁵¹ INFN, Laboratori Nazionali di Frascati, Frascati, Italy
- ⁵² INFN, Sezione di Bari, Bari, Italy
- ⁵³ INFN, Sezione di Bologna, Bologna, Italy
- ⁵⁴ INFN, Sezione di Cagliari, Cagliari, Italy
- ⁵⁵ INFN, Sezione di Catania, Catania, Italy
- ⁵⁶ INFN, Sezione di Padova, Padova, Italy
- ⁵⁷ INFN, Sezione di Roma, Rome, Italy
- ⁵⁸ INFN, Sezione di Torino, Turin, Italy
- ⁵⁹ INFN, Sezione di Trieste, Trieste, Italy
- ⁶⁰ Inha University, Incheon, Republic of Korea
- ⁶¹ Institut de Physique Nucléaire d'Orsay (IPNO), Institut National de Physique Nucléaire et de Physique des Particules (IN2P3/CNRS), Université de Paris-Sud, Université Paris-Saclay, Orsay, France
- ⁶² Institute for Nuclear Research, Academy of Sciences, Moscow, Russia
- ⁶³ Institute for Subatomic Physics, Utrecht University/Nikhef, Utrecht, Netherlands
- ⁶⁴ Institute for Theoretical and Experimental Physics, Moscow, Russia
- ⁶⁵ Institute of Experimental Physics, Slovak Academy of Sciences, Košice, Slovakia
- ⁶⁶ Institute of Physics, Homi Bhabha National Institute, Bhubaneswar, India
- ⁶⁷ Institute of Physics of the Czech Academy of Sciences, Prague, Czech Republic
- ⁶⁸ Institute of Space Science (ISS), Bucharest, Romania
- ⁶⁹ Institut für Kernphysik, Johann Wolfgang Goethe-Universität Frankfurt, Frankfurt, Germany
- ⁷⁰ Instituto de Ciencias Nucleares, Universidad Nacional Autónoma de México, Mexico City, Mexico
- ⁷¹ Instituto de Física, Universidade Federal do Rio Grande do Sul (UFRGS), Porto Alegre, Brazil
- ⁷² Instituto de Física, Universidad Nacional Autónoma de México, Mexico City, Mexico
- ⁷³ IThemba LABS, National Research Foundation, Somerset West, South Africa
- ⁷⁴ Johann-Wolfgang-Goethe Universität Frankfurt Institut für Informatik, Fachbereich Informatik und Mathematik, Frankfurt, Germany
- ⁷⁵ Joint Institute for Nuclear Research (JINR), Dubna, Russia
- ⁷⁶ Korea Institute of Science and Technology Information, Daejeon, Republic of Korea
- ⁷⁷ KTO Karatay University, Konya, Turkey
- ⁷⁸ Laboratoire de Physique Subatomique et de Cosmologie, Université Grenoble-Alpes, CNRS-IN2P3, Grenoble, France
- ⁷⁹ Lawrence Berkeley National Laboratory, Berkeley, CA, United States
- ⁸⁰ Lund University Department of Physics, Division of Particle Physics, Lund, Sweden
- ⁸¹ Nagasaki Institute of Applied Science, Nagasaki, Japan

- ⁸² Nara Women's University (NWU), Nara, Japan
- ⁸³ National and Kapodistrian University of Athens, School of Science, Department of Physics, Athens, Greece
- ⁸⁴ National Centre for Nuclear Research, Warsaw, Poland
- ⁸⁵ National Institute of Science Education and Research, Homi Bhabha National Institute, Jatni, India
- ⁸⁶ National Nuclear Research Center, Baku, Azerbaijan
- ⁸⁷ National Research Centre Kurchatov Institute, Moscow, Russia
- ⁸⁸ Niels Bohr Institute, University of Copenhagen, Copenhagen, Denmark
- ⁸⁹ Nikhef, National institute for subatomic physics, Amsterdam, Netherlands
- ⁹⁰ NRC Kurchatov Institute IHEP, Protvino, Russia
- ⁹¹ NRNU Moscow Engineering Physics Institute, Moscow, Russia
- ⁹² Nuclear Physics Group, STFC Daresbury Laboratory, Daresbury, United Kingdom
- ⁹³ Nuclear Physics Institute of the Czech Academy of Sciences, Řež u Prahy, Czech Republic
- ⁹⁴ Oak Ridge National Laboratory, Oak Ridge, TN, United States
- ⁹⁵ Ohio State University, Columbus, OH, United States
- ⁹⁶ Petersburg Nuclear Physics Institute, Gatchina, Russia
- ⁹⁷ Physics department, Faculty of science, University of Zagreb, Zagreb, Croatia
- ⁹⁸ Physics Department, Panjab University, Chandigarh, India
- ⁹⁹ Physics Department, University of Jammu, Jammu, India
- ¹⁰⁰ Physics Department, University of Rajasthan, Jaipur, India
- ¹⁰¹ Physikalisches Institut, Eberhard-Karls-Universität Tübingen, Tübingen, Germany
- ¹⁰² Physikalisches Institut, Ruprecht-Karls-Universität Heidelberg, Heidelberg, Germany
- ¹⁰³ Physik Department, Technische Universität München, Munich, Germany
- ¹⁰⁴ Research Division and ExtreMe Matter Institute EMMI, GSI Helmholtzzentrum für Schwerionenforschung GmbH, Darmstadt, Germany
- ¹⁰⁵ Rudjer Bošković Institute, Zagreb, Croatia
- ¹⁰⁶ Russian Federal Nuclear Center (VNIIEF), Sarov, Russia
- ¹⁰⁷ Saha Institute of Nuclear Physics, Homi Bhabha National Institute, Kolkata, India
- ¹⁰⁸ School of Physics and Astronomy, University of Birmingham, Birmingham, United Kingdom
- ¹⁰⁹ Sección Física, Departamento de Ciencias, Pontificia Universidad Católica del Perú, Lima, Peru
- ¹¹⁰ Shanghai Institute of Applied Physics, Shanghai, China
- ¹¹¹ St. Petersburg State University, St. Petersburg, Russia
- ¹¹² Stefan Meyer Institut für Subatomare Physik (SMI), Vienna, Austria
- ¹¹³ SUBATECH, IMT Atlantique, Université de Nantes, CNRS-IN2P3, Nantes, France
- ¹¹⁴ Suranaree University of Technology, Nakhon Ratchasima, Thailand
- ¹¹⁵ Technical University of Košice, Košice, Slovakia
- ¹¹⁶ Technische Universität München, Excellence Cluster 'Universe', Munich, Germany
- ¹¹⁷ The Henryk Niewodniczański Institute of Nuclear Physics, Polish Academy of Sciences, Cracow, Poland
- ¹¹⁸ The University of Texas at Austin, Austin, TX, United States
- ¹¹⁹ Universidad Autónoma de Sinaloa, Culiacán, Mexico
- ¹²⁰ Universidade de São Paulo (USP), São Paulo, Brazil
- ¹²¹ Universidade Estadual de Campinas (UNICAMP), Campinas, Brazil
- ¹²² Universidade Federal do ABC, Santo Andre, Brazil
- ¹²³ University College of Southeast Norway, Tonsberg, Norway
- ¹²⁴ University of Cape Town, Cape Town, South Africa
- ¹²⁵ University of Houston, Houston, TX, United States
- ¹²⁶ University of Jyväskylä, Jyväskylä, Finland
- ¹²⁷ University of Liverpool, Liverpool, United Kingdom
- ¹²⁸ University of Science and Technology of China, Hefei, China
- ¹²⁹ University of Tennessee, Knoxville, TN, United States
- ¹³⁰ University of the Witwatersrand, Johannesburg, South Africa
- ¹³¹ University of Tokyo, Tokyo, Japan
- ¹³² University of Tsukuba, Tsukuba, Japan
- ¹³³ Université Clermont Auvergne, CNRS/IN2P3, LPC, Clermont-Ferrand, France
- ¹³⁴ Université de Lyon, Université Lyon 1, CNRS/IN2P3, IPN-Lyon, Villeurbanne, Lyon, France
- ¹³⁵ Université de Strasbourg, CNRS, IPHC UMR 7178, F-67000, Strasbourg, France
- ¹³⁶ Université Paris-Saclay Centre d'Études de Saclay (CEA), IRFU, Department de Physique Nucléaire (DPhN), Saclay, France
- ¹³⁷ Università degli Studi di Foggia, Foggia, Italy
- ¹³⁸ Università degli Studi di Pavia, Pavia, Italy
- ¹³⁹ Università di Brescia, Brescia, Italy
- ¹⁴⁰ Variable Energy Cyclotron Centre, Homi Bhabha National Institute, Kolkata, India
- ¹⁴¹ Warsaw University of Technology, Warsaw, Poland
- ¹⁴² Wayne State University, Detroit, MI, United States
- ¹⁴³ Westfälische Wilhelms-Universität Münster, Institut für Kernphysik, Münster, Germany
- ¹⁴⁴ Wigner Research Centre for Physics, Hungarian Academy of Sciences, Budapest, Hungary
- ¹⁴⁵ Yale University, New Haven, CT, United States
- ¹⁴⁶ Yonsei University, Seoul, Republic of Korea

ⁱ Deceased.

ⁱⁱ Dipartimento DET del Politecnico di Torino, Turin, Italy.

ⁱⁱⁱ M.V. Lomonosov Moscow State University, D.V. Skobeltsyn Institute of Nuclear, Physics, Moscow, Russia.

^{iv} Department of Applied Physics, Aligarh Muslim University, Aligarh, India.

^v Institute of Theoretical Physics, University of Wrocław, Poland.